Quaternary Science Reviews 219 (2019) 297–307

Contents lists available at ScienceDirect

Quaternary Science Reviews

journal homepage: www.elsevier.com/locate/quascirev

Extreme hydroclimate response gradients within the western Cape Floristic region of South Africa since the Last Glacial Maximum

Brian M. Chase [a, *], Arnoud Boom [b], Andrew S. Carr [b], Manuel Chevalier [c], Lynne J. Quick [d], G. Anthony Verboom [e], Paula J. Reimer [f]

[a] Institut des Sciences de l'Evolution-Montpellier (ISEM), University of Montpellier, Centre National de la Recherche Scientifique (CNRS), EPHE, IRD, Montpellier, France
[b] School of Geography, Geology and the Environment, University of Leicester, Leicester, LE1 7RH, UK
[c] Institute of Earth Surface Dynamics, Geopolis, University of Lausanne, Quartier UNIL-Mouline, Bâtiment Géopolis, CH-1015 Lausanne, Switzerland
[d] African Centre for Coastal Palaeoscience, Nelson Mandela University, 6031 Port Elizabeth, South Africa
[e] Department of Biological Sciences, University of Cape Town, 7700 Rondebosch, South Africa
[f] School of Natural and Built Environment, Queen's University Belfast, Belfast, BT7 1NN, Northern Ireland, UK

ARTICLE INFO

Article history:
Received 17 May 2019
Received in revised form
6 July 2019
Accepted 6 July 2019

Keywords:
Palaeoclimate
Climate dynamics
South Africa
Cape Floristic region
Biodiversity
Rock hyrax middens
Stable isotopes

ABSTRACT

The Cape Floristic Region (CFR) is one of the world's major biodiversity hotspots, and much work has gone into identifying the drivers of this diversity. Considered regionally in the context of Quaternary climate change, climate stability is generally accepted as being one of the major factors promoting the abundance of species now present in the CFR. However, little direct evidence is available from the region, and responses to changes in global boundary conditions have been difficult to assess. In this paper, we present new high-resolution stable isotope data from Pakhuis Pass, in the species-rich western CFR, and contextualise our findings through comparison with other records from the region. Combined, they indicate clear, coherent changes in regional hydroclimate, which we relate to broader forcing mechanisms. However, while these climate change events share similar timings (indicating shared macro-scale drivers), the responses are distinct between sites, in some cases expressing opposing trends over very short spatial gradients (<50 km). We describe the evolution of these trends, and propose that while long-term (10^5 yr) general climatic stability may have fostered high diversity in the region through low extinction rates, the strong, abrupt changes in hydroclimate gradients observed in our records may have driven a form of allopatric speciation pump, promoting the diversification of plant lineages through the periodic isolation and recombination of plant populations.

1. Introduction

Southern African hydroclimate is primarily defined by the advection and precipitation of moisture from tropical Atlantic and Indian Ocean sources during the austral summer (Fig. 1). In contrast, southwestern South Africa experiences a distinct, inverse rainfall regime. Seasonal expansions of the circumpolar vortex and equatorward migration of the westerly storm track bring increased precipitation during winter months, while displacements of the South Atlantic Anticyclone during the summer intensify upwelling along the west coast, blocking the westward propagation of easterly waves, generating strong summer drought in the region (Tyson, 1986; Tyson and Preston-Whyte, 2000). During the Quaternary, southern Africa is thought to have been sensitive to long-term changes in these tropical and temperate systems. Driven by changes in global boundary conditions, tropical systems are invigorated during interglacial periods and temperate systems exert increased influence during glacial periods (Chase et al., 2015a; Chase et al., 2017; see Chase and Meadows, 2007; Cockroft et al., 1988; Quick et al., 2011; van Zinderen Bakker, 1976).

This dynamic, which is thought to have become dominant in the Plio-Pleistocene (5.0–2.6 Ma) when trade wind-controlled upwelling was established as a dominant factor in the regional climate system (Diekmann et al., 2003), has created a Mediterranean climate zone in the southwestern Cape of South Africa (Fig. 2). This climatic evolution has been a key factor in fostering the

* Corresponding author.
E-mail address: Brian.Chase@umontpellier.fr (B.M. Chase).

https://doi.org/10.1016/j.quascirev.2019.07.006
0277-3791/

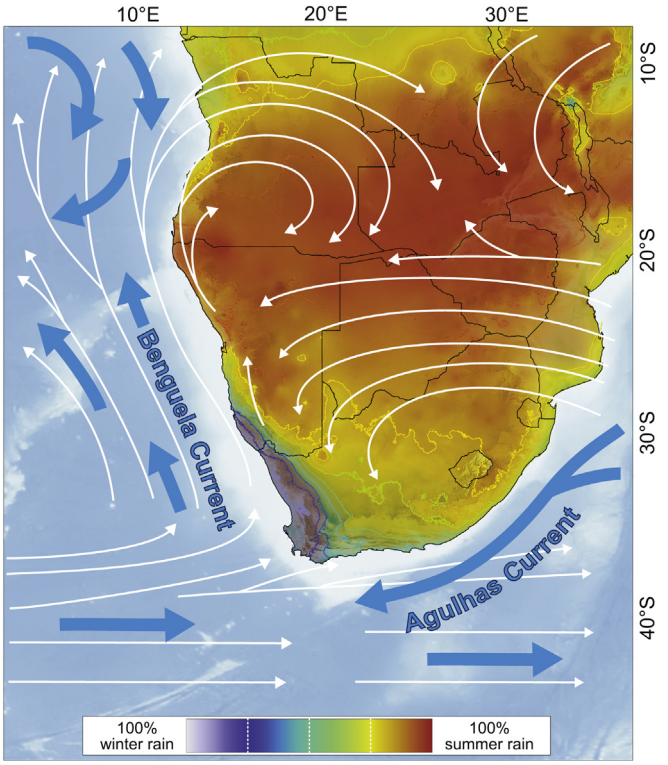

Fig. 1. Map of southern Africa showing seasonality of rainfall and climatic gradients dictated by the zones of summer/tropical (red) and winter/temperate (blue) rainfall dominance. Major atmospheric (white arrows) and oceanic (blue arrows) circulation systems are indicated. (For interpretation of the references to colour in this figure legend, the reader is referred to the Web version of this article.)

development of the vegetation of the Cape Floristic Region (CFR), which is remarkable for its high level of endemism and its species richness (Cowling, 1992; Goldblatt, 1978).

It has been recognised, however, that species diversity within the CFR, is not homogeneous, with the winter-rain dominated western CFR having more than twice the species per area of the eastern CFR, which currently experiences an aseasonal rainfall regime (Fig. 2) (Cowling et al., 1992, 1997; Cowling and Lombard, 2002). During the Quaternary, the western CFR has putatively experienced a continuous dominance of temperate systems, whereas the eastern CFR rainfall regimes may have oscillated between temperate and tropical rainfall dominance (see Chase and Meadows, 2007) with much more significant consequences on the distribution and nature of environmental niches (Cowling et al., 1992, 1999). With a reliable climate regime, and relatively muted cycles of Quaternary climate change compared to the extratropical regions in the Northern Hemisphere (see Chase and Meadows, 2007; Dynesius and Jansson, 2000), it is believed that the CFR's great floral diversity – particularly in the west – is largely attributable to relative climatic stability and resulting low extinction rates (Cowling et al., 1992, 1997, 2015; Cowling and Lombard, 2002; Linder, 2005; Verboom et al., 2014). These hypotheses, and the conclusion that the western CFR represented a more durable climatic niche than the eastern CFR is supported by analyses of phylogenetic diversity, which indicate that the western CFR experienced higher levels of in situ radiation, while the eastern CFR indicates significant mixing of lineages from different biomes (Forest et al., 2007; Verboom et al., 2014).

At broad spatio-temporal scales, it thus seems apparent that the development of, and the dynamics within, the southwestern Cape's Mediterranean climate region were fundamental determinants for the evolution of the CFR. At finer spatial and temporal scales, these considerations become more complex. In the western CFR, it has been observed that species richness is higher in the mountains than the lowlands, a situation related to topographic variability and the resulting diversity of edaphic and climate spaces (Linder, 1991; Verboom et al., 2015). Linder (1991) also found that species richness correlated most strongly with mean annual precipitation, which might further suggest that climatic stability is a key determinant of species diversity (as regions of currently high rainfall may be acting as interglacial refugia for many CFR taxa (Chase and Meadows, 2007; Forest et al., 2007)). But how stable were climates in these montane regions?

In this paper, we consider the climatic context of the high-diversity montane regions of the western CFR in the light of new, high resolution palaeoclimatic data obtained from the region. While neither spatially nor temporally comprehensive, it does enable the beginnings of a more detailed analysis and understanding of the nature of climate change dynamics in the region. While some studies have suggested long-term millennial-scale climate and vegetation stability (Meadows et al., 2010; Meadows and Sugden, 1991), a growing body of data indicates potentially more dynamic patterns of climate change, and further indicates that spatial climate gradients may be much more complex than previously supposed (Chase et al., 2011, 2015a). To address this, we present a new 19,300-year stable isotope composite record derived from rock hyrax middens from Pakhuis Pass in the Cederberg Mountains. Considered together with the records from other hyrax midden records from De Rif (Chase et al., 2011, 2015a) and Katbakkies Pass (Chase et al., 2015b; Meadows et al., 2010), we are able to assess the spatio-temporal dynamics of climate change along a modern climatic gradient in the Cape Fold Belt Mountains of the western CFR – across the eastern slope of the Cederberg, and determine to what extent regional climates can be considered to be stable.

1.1. Regional setting

Pakhuis Pass is located in the northern Cederberg Mountains, the dominant range of the north-south axis of the Cape Fold Mountains to the east and northeast of Cape Town (Figs. 2 and 3). Extending for ~200 km parallel to the Atlantic Ocean (50–100 km to the west), this western limb of the Cape Fold Belt is a significant divide between the relatively humid climates of the southwestern Cape and the arid Karoo, which dominates much of South Africa's western continental interior. The range also broadly marks the divide between southern Africa's two major climate regimes: the winter rainfall zone (WRZ) to the west and the summer rainfall zone (SRZ) to the northeast (cf. Chase and Meadows, 2007). The winter rainfall zone is defined by the seasonal intensification and northward expansion of the westerlies and associated frontal depressions that transport moisture to the region during the austral winter months. To the east, and across most of South Africa, tropical easterly flow transports moisture from the Indian Ocean during the austral summer. The Cederberg and adjacent ranges act as an orographic divide between these climate zones, with the mountains creating a distinct rainshadow for westerly derived rainfall (Fig. 3; Tyson, 1986; Tyson and Preston-Whyte, 2000). The higher elevations receive five times the precipitation of the lowlands to the east, but perhaps more importantly, while the Cederberg Mountains receive more than 75% of their rainfall during the winter, the lowlands to the east currently receive 50% or more of their precipitation during the summer (Hijmans et al., 2005) (Fig. 1).

Pakhuis Pass is located at ~485 m.a.s.l. on the eastern slopes of the Cederberg, in the rainshadow of the Pakhuisberge massif

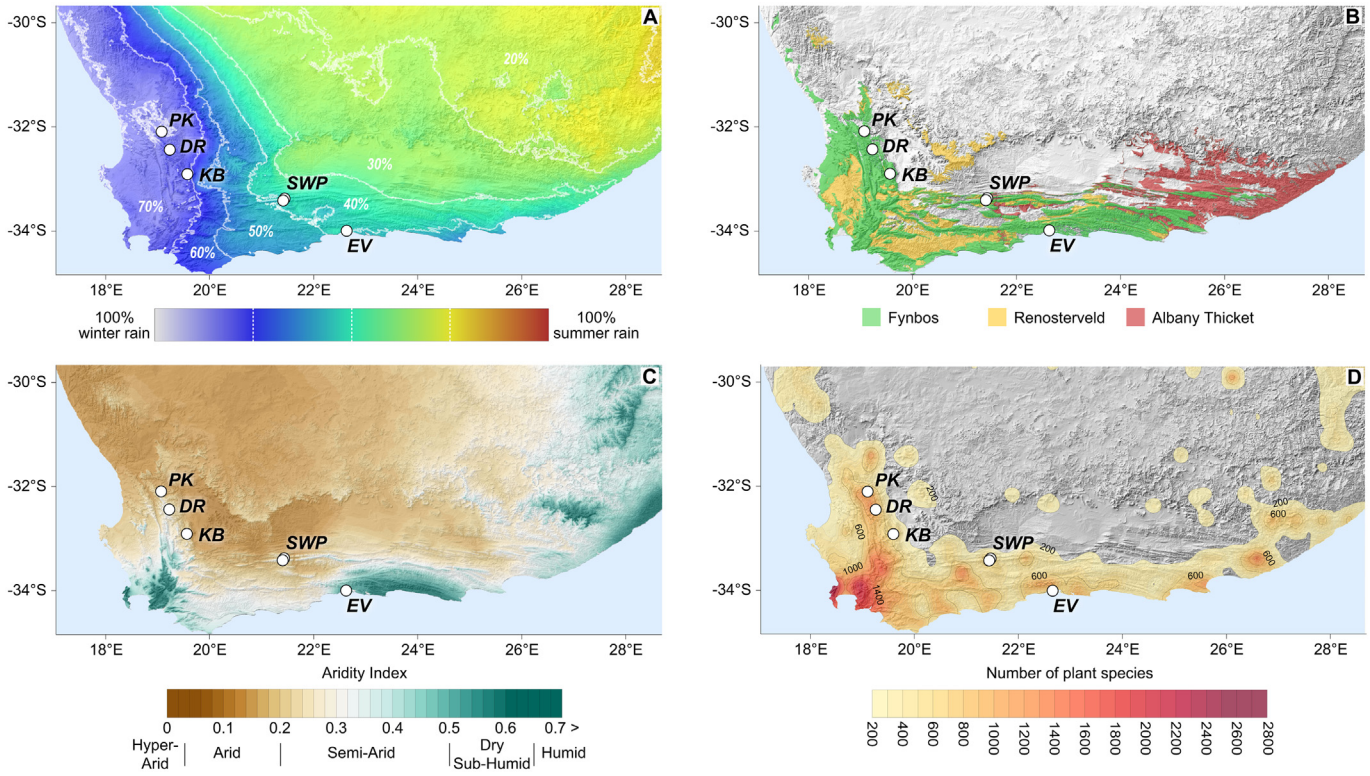

Fig. 2. Map of southernmost Africa showing A) showing seasonality of rainfall and climatic gradients defined in terms of percentage of winter rainfall, B) the extent of the vegetation types comprising the Cape Floristic Region (fynbos, renosterveld and Albany Thicket (data from Mucina and Rutherford, 2006)), C) a map of mean Aridity Index values for the region (Trabucco and Zomer, 2009), and D) a map of species richness using data derived from the GBIF database (Chevalier, 2019, 2018; GBIF.org, 2018a, b, c, d, e, f, g, h, i); number of species per quarter-degree grid cell were interpolated to create the contour map. Classification of aridity values follows that of the UNEP (United Nations Environment Programme, 1997). Sites considered in this study are indicated: Pakhuis Pass (PK: this study; Scott and Woodborne, 2007a; Scott and Woodborne, 2007b), De Rif (DR: Chase et al., 2015a; Chase et al., 2011; Quick et al., 2011), Katbakkies Pass (KB: Chase et al., 2015b; Meadows et al., 2010), Seweweekspoort (SWP: Chase et al., 2015a; Chase et al., 2013; Chase et al., 2017) and Eilandvlei (Quick et al., 2018).

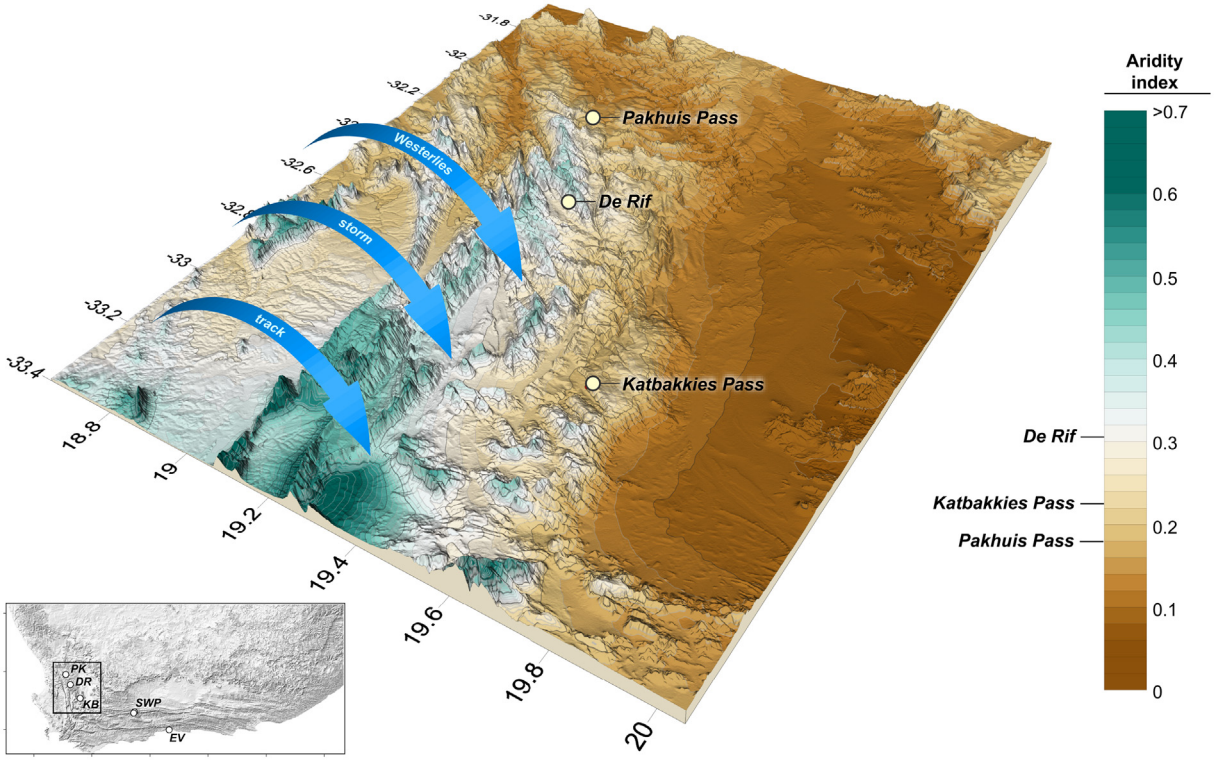

Fig. 3. Map of the N-S axis of the Cape Fold Mountains in the southwestern Cape, including the Cederberg Mountains and adjacent ranges. Topographic variability (MERIT digital elevation model; Yamazaki et al., 2017) is overlain by a map of mean Aridity Index values (Trabucco and Zomer, 2009) for the region, as in Fig. 1. The dominant vector of temperate moisture-bearing systems related to the westerly storm track is shown, as are the sites considered in this study: Pakhuis Pass (this study; Scott and Woodborne, 2007a; Scott and Woodborne, 2007b), De Rif (Chase et al., 2011, 2015a; Quick et al., 2011), Katbakkies Pass (Chase et al., 2015b; Meadows et al., 2010). The relative aridity of each sites is shown on the legend. Inset indicates position of the region within the southwestern Cape.

(~1000 m.a.s.l.) (Fig. 3). Mean annual rainfall at the site is ~250–300 mm/yr, ~80% of which falls in the austral winter between April and September (Hijmans et al., 2005). In comparison, the hyrax midden sites at De Rif (Chase et al., 2011, 2015a; Quick et al., 2011) and Katbakkies Pass (Chase et al., 2015b; Meadows et al., 2010) (Figs. 2 and 3) are both situated at ~1150 m.a.s.l., receive ~400 mm/yr and ~300 mm/yr of mean annual rainfall respectively, and by virtue of their elevation and position relative to the region's major topographic features they are more likely to receive precipitation during the summer months through orographic amplification of local or larger synoptic-scale systems (Tyson, 1986; Tyson and Preston-Whyte, 2000).

2. Material and methods

Middens for this study, PK08 and PK10-1 (Fig. 4) were collected from the same ~400 m long, 15 m high cliff band (32.093°S, 19.065°E) as those described by Scott and Woodborne (2007a, b) and were selected for their high hyraceum (crystallised urine) relative to faecal pellet content. Apart from having greater structural integrity and less variable deposition rates, hyraceum represents environmental conditions more clearly than samples containing faecal pellets, which may potentially include a degree of dietary bias and often exhibit far more discontinuous/irregular deposition (Chase et al., 2012). Sections of each midden were cut perpendicular to the stratigraphy using an angle grinder and/or

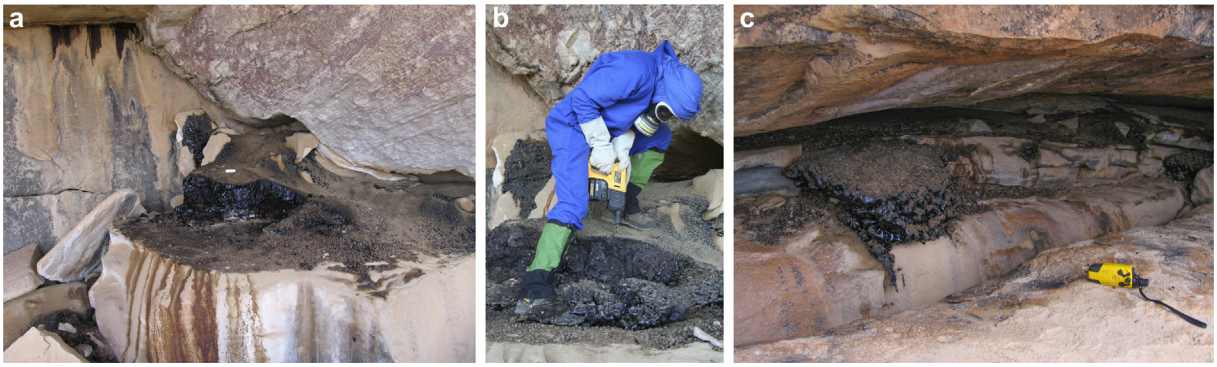

Fig. 4. Pakhuis Pass rock hyrax middens sampled for this study: a) PK08, 7 cm tool atop midden for scale; b) collecting a portion of the PK08 midden; c) PK10-1 midden, 16 cm GPS unit for scale.

Table 1
Radiocarbon ages and calibration information for the PK08, PK10-1 and PK1173 (Scott and Woodborne, 2007a, b) rock hyrax middens.

Sample	Depth (mm)	^{14}C age yr BP	1 sigma error	calibration data	95.4% (2σ) cal age ranges		relative area under distribution	median probability (cal BP)
					lower cal range BP	upper cal range BP		
PK08								
UBA-9442	14.1146	1732	21	SHCal13	1538	1618	0.761729	1591
					1654	1698	0.238271	
UBA-19733	20.5208	2317	28	SHCal13	2164	2167	0.00474	2311
					2178	2265	0.414168	
					2297	2352	0.581093	
UBA-20527	42.5000	3220	37	SHCal13	3255	3292	0.049469	3403
					3328	3481	0.943047	
					3537	3546	0.007484	
UBA-18630	74.4792	4346	32	SHCal13	4828	4968	1	4866
UBA-18631	106.3021	5326	42	SHCal13	5935	6187	1	6071
UBA-19734	122.3958	5411	44	SHCal13	6003	6085	0.258572	6157
					6095	6280	0.741428	
UBA-18632	164.2708	6224	44	SHCal13	6949	7180	0.941196	7081
					7194	7241	0.058804	
UBA-18633	202.1875	7642	58	SHCal13	8221	8236	0.009215	8405
					8309	8544	0.990785	
PK10-1								
UBA-16733	8.8188	1253	24	SHCal13	1059	1185	1	1126
UBA-18634	29.7356	8311	51	SHCal13	9036	9047	0.010375	9260
					9088	9431	0.989625	
UBA-18635	79.0508	11962	66	SHCal13	13564	13965	1	13741
UBA-18636	123.6223	13931	78	SHCal13	16503	17108	1	16825
UBA-18637	169.1808	15392	90	SHCal13	18397	18807	1	18621
UBA-16734	188.0282	15558	69	SHCal13	18612	18918	1	18774
PK1173								
Pta-5896	25.0	13000	130	SHCal13	15123	15908	1	15498
Pta-5737	75.0	13850	130	SHCal13	16281	17109	1	16704
Pta-5897	120.0	14470	140	SHCal13	17181	17936	1	17579
Pta-5895	159.0	15200	120	SHCal13	18088	18694	1	18414
Pta-5882	196.0	15800	160	SHCal13	18702	19454	1	19032

rotary impact hammer (Fig. 4) and transported back to the laboratory for analysis. In addition to these newly collected middens, we analysed one of the Pakhuis Pass middens (PK1173) considered in the papers of Scott and Woodborne (2007a, b).

2.1. Chronology

Radiocarbon age determinations for the PK08 and PK10-1 middens (n = 14) were processed at the ^{14}CHRONO Centre, Queen's University Belfast using accelerator mass spectrometry (AMS) (Table 1; Fig. 5). Samples were pre-treated with 2% HCl for 1 h at room temperature to remove carbonates and dried at 60 °C. They were then weighed into quartz tubes with an excess of CuO, sealed under vacuum and combusted to CO_2. The CO_2 was converted to graphite on an iron catalyst using the zinc reduction method (Slota et al., 1987). The radiocarbon ages were corrected for isotope fractionation using the AMS measured δ^{13}C. These ages and those obtained from PK1173 (Scott and Woodborne, 2007a) were calibrated using the SHCal13 calibration data (Hogg et al., 2013). The Clam 2.2 software package (Blaauw, 2010) was used to generate all age-depth models (Fig. 5). Clam was chosen over Bayesian techniques such as Bacon (Blaauw and Christen, 2011) because strong changes in accumulation rate may occur in hyrax middens (such as PK08 and PK10-1), and Clam – using linear models - is better suited to such sequences.

2.2. Stable nitrogen isotopes

Stable nitrogen isotope analysis of midden hyraceum samples were performed at the Department of Archaeology, University of Cape Town following Chase et al. (2010, 2009), with a contiguous/overlapping samples obtained two series of offset 1 mm holes. The standard deviation derived from replicate analyses of homogeneous material was better than 0.2‰. Results are expressed relative to atmospheric nitrogen.

3. Results

3.1. Chronology

Radiocarbon analyses indicate that the Pakhuis Pass hyrax middens accumulated during the late Pleistocene and Holocene, spanning the last ~19,300 years cal (calibrated) BP. The age-depth models for the two middens suggest continuous deposition, although accumulation rates do vary considerably (Table 1; Fig. 5). Accumulation rates for the PK08 midden average ~28 μm yr^{-1}, with a period of more rapid accumulation centred on 6000 cal BP (~132 μm yr^{-1}). Each 1 mm isotope sample from PK08 therefore integrates between ~8 and 105 years of hyraceum accumulation (averaging 42 mm/yr). Accumulation rates for the PK10-1 midden increase with age/depth, from ~2.6 μm yr^{-1} in the uppermost 30 mm to ~106 μm yr^{-1} in the bottom 13 mm. Therein, each 1 mm isotope sample from PK10-1 integrates between ~380 years (upper section) to ~10 years (lower section) of hyraceum accumulation. Because of this significant change in accumulation rate, we show data from the extremely low resolution of the Holocene portion of PK10-1, but do not consider it in our analyses, favouring the much more highly resolved record from PK08. Accumulation of the PK1173 midden (Scott and Woodborne, 2007a) was more regular, averaging ~50 μm yr^{-1}, with each isotope sample integrating ~20 years of accumulation.

3.2. Stable nitrogen isotopes

The δ^{15}N values from the PK08, PK10-1 and PK1173 middens vary from 3.6 to 8.6‰ (Fig. 6). Variations in midden δ^{15}N are interpreted to reflect changes in water availability (see more extensive discussion in Chase et al., 2012). At the global scale, a relationship has been recognised between aridity and foliar ^{15}N (e.g. Craine et al., 2009; Hartman and Danin, 2010), and replication of this signal in plant and animal tissues and in faecal matter (e.g. Carr et al., 2016; Hartman, 2011; Murphy and Bowman, 2006; Newsome et al., 2011) has been demonstrated. This is thought to be generally a function of a more open nitrogen cycle in arid regions. Fractionating pathways in the soil (nitrification, denitrification,

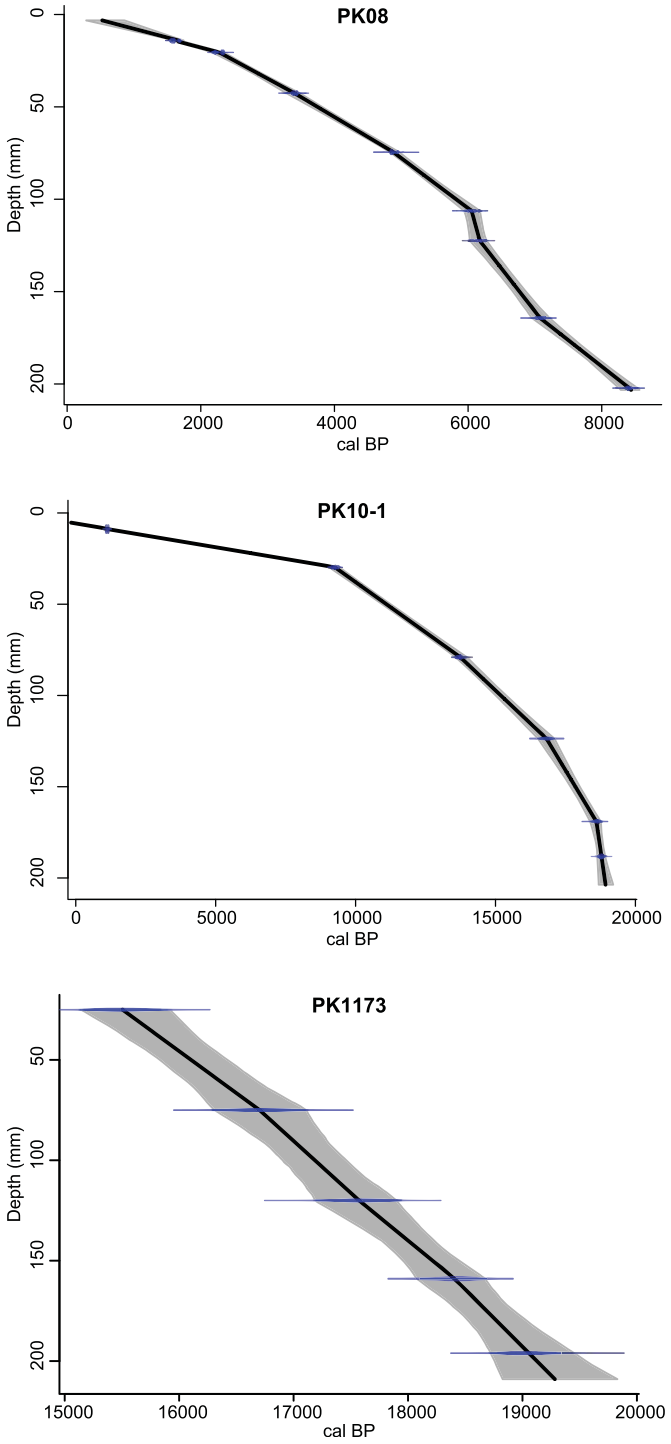

Fig. 5. Age-depth models for the PK08, PK10-1 and PK1173 rock hyrax middens.

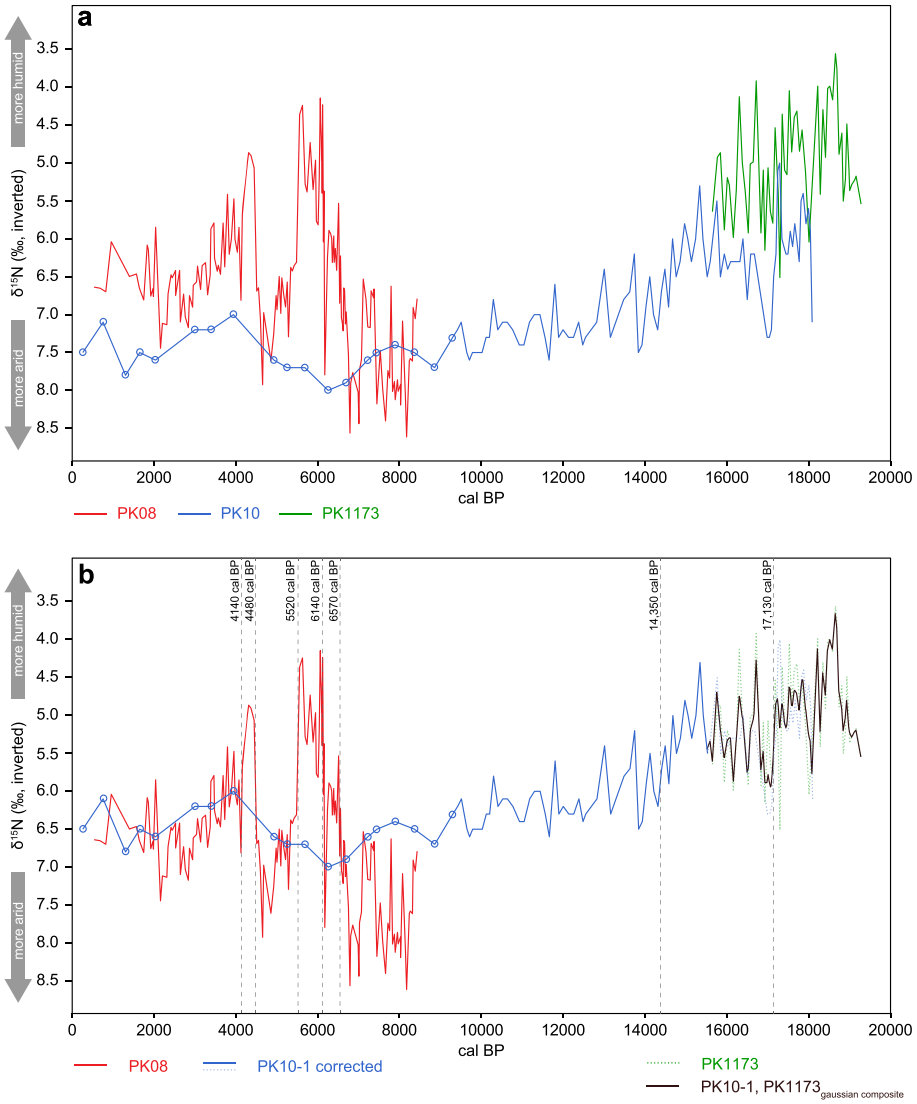

Fig. 6. Pane (a): The $\delta^{15}N$ data from the PK08 (red), PK10-1 (blue, sample location provided for lower resolution Holocene portion) and PK1173 (green) rock hyrax middens. Pane (b): The same records following corrections made to establish a single composite record for the site. The PK10-1 midden is associated with a more exposed foraging range and thinner soils, and a 0.95‰ correction factor was applied based on average values from PK08 and PK1173 (recovered from more mesic locations) for overlapping time periods. For the >15,500 cal BP portion of the sequence the similarly resolved, but irregularly sampled overlapping portions of PK10-1 and PK1173 (dashed lines) have been combined (shown in black) using Gaussian kernel-based interpolation (Rehfeld et al., 2011). The timing of major changes as identified from the composite record using change point analysis (Killick et al., 2012) are indicated by vertical dashed lines. (For interpretation of the references to colour in this figure legend, the reader is referred to the Web version of this article.)

etc.) mean that nitrogen lost through transformation and the release of gaseous products is depleted in ^{15}N, and the remaining nitrogen is enriched. While in more humid regions N is cycled between live and dead organic pools, in drier regions more N flows to mineral pools where it is subject to gaseous loss (Amundson et al., 2003), and the $\delta^{15}N$ value of soils is thus higher with increasing aridity (Austin and Vitousek, 1998; Handley et al., 1999; Murphy and Bowman, 2009). The environmental processes relating to this recycling or loss of ^{15}N are not tied exclusively to rainfall amount, but in climatic terms are more accurately considered to relate to water availability (Murphy and Bowman, 2006). Studies of ^{15}N in hyrax middens from a wide range of environments indicate consistently strong correlations between midden ^{15}N, local vegetation/soil 15N, as well as independent climate proxy records, supporting the conclusion that environmental moisture availability is a major driver of midden ^{15}N records (Carr et al., 2016; Chase et al., 2009, 2010, 2011, 2013, 2015a, 2015b, 2017).

This general relationship may also be influenced to some extent by other (e.g. microclimatic) factors, as is reflected in the variability observed in the relationship between modern foliar ^{15}N and aridity estimates (e.g. Hartman and Danin, 2010; Murphy and Bowman, 2006; Peri et al., 2012). This influence can be observed in the offset between the PK08 and PK1173 records and the record from PK10-1 (Fig. 6). This is not uncommon when comparing records from different middens, even when in relatively close proximity (<20 m) (Chase et al., 2013). These differences are believed to be driven by micro-topographic variations influencing water-availability in the primary feeding zones associated with each shelter (cf. Chase et al., 2013; Chase et al., 2017). In the case of the Pakhuis Pass middens, PK10-1 was retrieved from a narrow upper tier of the cliff complex, where the primary foraging range was likely to have been dominated by plants able to establish in the exposed landscape and thin soils found on the rock shelves above the cliff. PK08 and PK1173, in contrast, are located near the cliff base, and surrounded by deeper soils and higher groundwater recharge potential, which supports a more mesic, denser

vegetation. The result is that while trends in $\delta^{15}N$ variability are similar between the PK08, PK1173 and PK10-1 middens, the PK10-1 values are approximately 0.95‰ higher (established by comparison of average values for the overlapping sections of midden sequences). For combination and consideration of the records, we have applied a 0.95‰ correction factor to the PK10-1 data.

To create a single composite record, we selected the PK08 record over the much lower resolution PK10-1 record for the mid-to late Holocene, as the latter is little informative in this context, with greater temporal averaging attenuating the variability evident in the higher resolution PK08 record. For the late Pleistocene, PK10-1 and PK1173 are of similar resolution and indicate similar trends. To incorporate information from both middens, we combined and smoothed the age-ranked data ensemble using Gaussian kernel-based interpolation (Rehfeld et al., 2011). This technique has been shown to be the most appropriate to interpolate irregularly sampled time series. We followed the recommendation of Rehfeld et al. (2011) and used the average temporal resolution of the data from these sections (31.97 years) to define the width of our Gaussian kernel. To maintain the true temporal resolution of our composite record, the values were interpolated at the sample ages.

As a whole, the Pakhuis Pass $\delta^{15}N$ data indicate a general aridification at the site (change towards higher $\delta^{15}N$ values) from the late Pleistocene to the Holocene (Fig. 6). The most humid periods recorded occur during the last glacial period, between 19,300 and 15,300 cal BP, and from 6100 to 5500 cal BP, following the early to mid-Holocene transition. Maximum aridity is reached during the early Holocene. The length and resolution of the records do not allow for definitive comparisons, but variability during the Pleistocene portion of the record – even considering its lower resolution - appears relatively muted compared to the strong, abrupt changes apparent in the Holocene.

Using change point analysis (Killick et al., 2012; Trauth et al., 2018), major transitions in the mean climate state (not accounting for changes in variability) in the record (where the root-mean-square level of the signal changes most significantly) were identified. Most notably, the period following the termination of early Holocene aridity at ~6800 cal BP is marked by a series of abrupt changes reflecting a rapid increase in water availability between ~6800 and 6140 cal BP. This period of relatively humid conditions ends equally abruptly, with distinctly drier conditions persisting from 5520 to 4480 cal BP. A subsequent sharp increase in water availability is followed by a gradual aridification between 4480 and 2830 cal BP, and apparently more stable conditions during the late Holocene. It is worth noting that the amplitude of change registered across these transitions (as much as 4.5‰) is similar to the amplitude of change between the Last Glacial Maximum and Holocene (5‰). Using the data derived from modern hyrax faecal pellets presented by Carr et al. (2016), this may speculatively be translated to a ~70% increase in water availability (Aridity Index from 0.25 to 0.42) for the period between ~6800 and 6100 cal BP (Fig. 6). Unfortunately, the midden records obtained do not provide detailed information regarding modern/sub-modern conditions, and a full contextualisation of these results in comparison with modern climates and recent change is not yet possible.

4. Discussion

4.1. Glacial-interglacial scale variability

Considering the combined influences of lower Pleistocene temperatures (Chevalier and Chase, 2016; Lim et al., 2016; Stute and Talma, 1998; Talma and Vogel, 1992), and the position of Pakhuis Pass in the winter rainfall zone, which is considered to have received increased precipitation during glacial periods (Chase et al., 2017; Chase and Meadows, 2007; Cockcroft et al., 1987; van Zinderen Bakker, 1976), it is not surprising that the late Pleistocene is characterised by more humid conditions (Fig. 7). What is most remarkable about the Pakhuis Pass $\delta^{15}N$ record is that it indicates dramatically different patterns of change than those recorded at De Rif hyrax midden site, located only 42 km to the south (Figs. 2 and 3; Chase et al., 2011, 2015). This implies past climate change dynamics characterised by marked levels of spatio-temporal heterogeneity. Previously, inter-regional differences have been indicated by $\delta^{15}N$ records from Seweweekspoort (Fig. 2; 230 km east-southeast of De Rif). In isolation, the differences between De Rif and Seweweekspoort might otherwise have been explained by the distinct natures of eastern and western CFR climate histories (Chase and Meadows, 2007; Cowling et al., 1992). The new data from Pakhuis Pass imply a more complex dynamic.

Interpretations of the Seweweekspoort and De Rif records, which extend into the Last Glacial Maximum (LGM; 19–26.5 ka (Clark et al., 2009)) have highlighted the influence of different elements of the regional climate system as they were impacted by changing global boundary conditions. At glacial-interglacial timescales, the $\delta^{15}N$ record from Seweweekspoort (Chase et al., 2017) has been identified as primarily reflecting changes in the climate

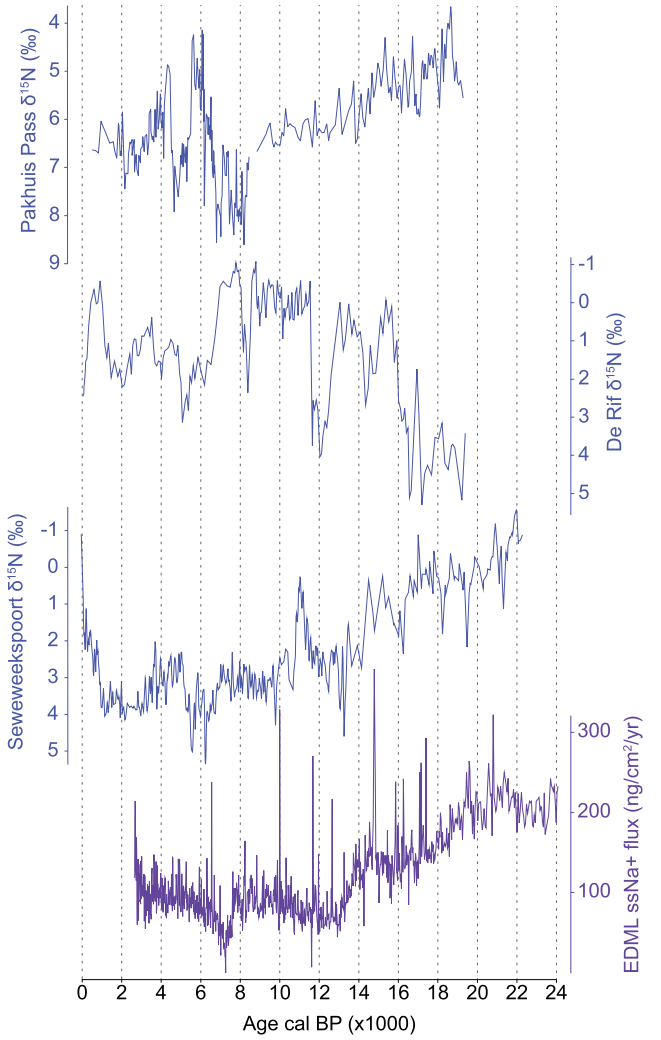

Fig. 7. The $\delta^{15}N$ data from the Pakhuis Pass (this paper), De Rif (Chase et al., 2011) and Seweweekspoort (Chase et al., 2017) rock hyrax middens, and the sea-salt sodium flux data from the EPICA Dronning Maud Land ice core from Antarctica, a proxy for sea-ice extent (Fischer et al., 2007).

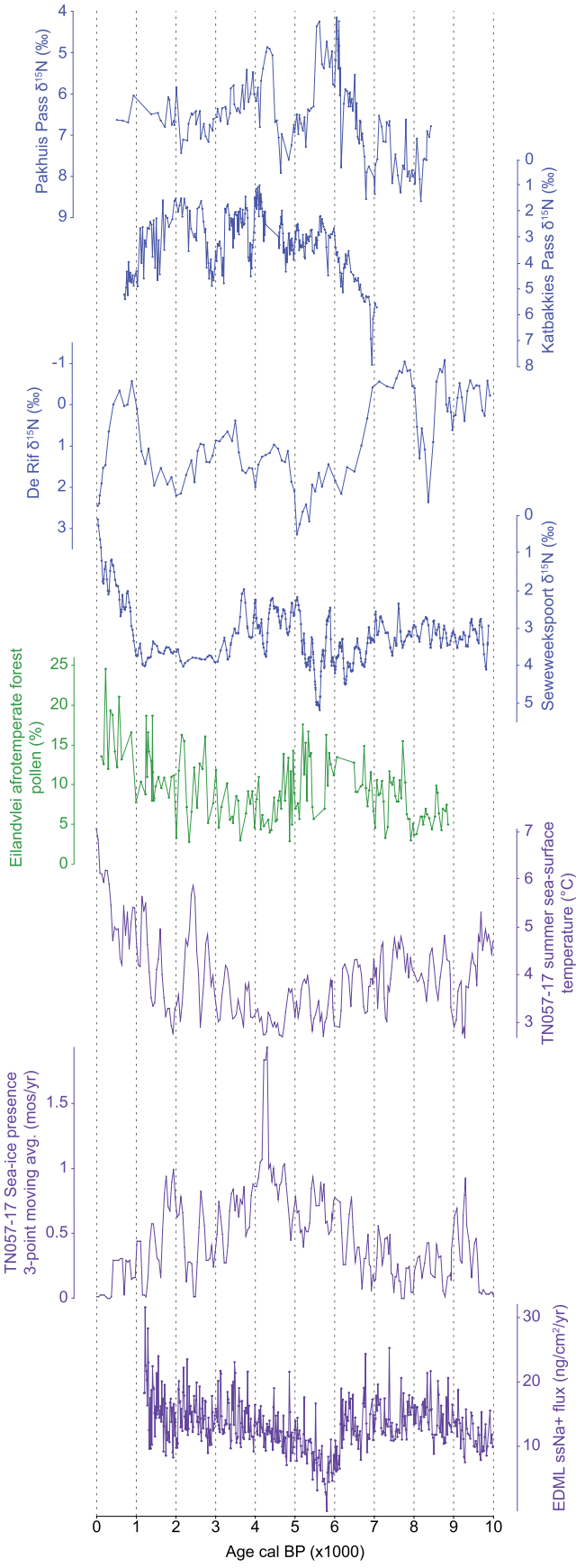

Fig. 8. Holocene $\delta^{15}N$ records from the Pakhuis Pass (this paper), Katbakkies Pass (Chase et al., 2015b), De Rif (Chase et al., 2015a) and Seweweekspoort (Chase et al., 2017) rock hyrax middens, as well as the afrotemperate forest pollen record from Eilandvlei (Quick et al., 2018), and proxies records relating to the position of the southern westerlies, including reconstructions of Southern Ocean summer sea-surface temperatures and sea ice presence (Nielsen et al., 2004) and the sea-salt sodium flux data from the EPICA Dronning Maud Land ice core from Antarctica, a proxy for sea-ice extent (Fischer et al., 2007; Roberts et al., 2017).

system related to global temperature and Antarctic sea-ice, which has been hypothesised as being a significant control on the position of the southern westerlies storm track (Chase and Meadows, 2007; Cockcroft et al., 1987; van Zinderen Bakker, 1976). In contrast, at De Rif, despite being closer to the core of the WRZ, where temperate systems define the modern regional rainfall regime, the primary control on hydrologic balance at millennial and multi-millennial timescales appears to be variations in the length and intensity of the summer drought season, potentially modulated by variations in the intensity of the South Atlantic Anticyclone, which blocks the incursion of tropical air masses and limits convection (Chase et al., 2015a). In the higher elevations of the Cederberg mountains, while winter rainfall is consistent and abundant, changes in summer rainfall may have had a more significant influence on driving drought-stress at the site. Including the new Pakhuis Pass $\delta^{15}N$ record in this regional consideration, it seems likely (based on similarities in first-order trends with SWP, as well as EPICA Dronning Maud Land ice core sea-salt sodium flux record, considered as a general proxy for sea-ice extent (Fischer et al., 2007)) that at glacial-interglacial timescales conditions at Pakhuis Pass is predominantly impacted by changes in temperate system influence, with summer rainfall playing a relatively limited role in defining water availability.

4.2. The Holocene

Focussing on the Holocene, more, and more precise data can be brought to bear on the question of CFR climate dynamics. While data coverage remains far from comprehensive, high resolution stable isotope data from rock hyrax middens have provided important clues as to some of the drivers and spatial dynamics that have defined climate change in the region during the Holocene (Fig. 8). Building from the basis of the conceptual models developed by van Zinderen Bakker (1976) and Cockcroft et al. (1987), which indicate that periods of global cooling (warming) will generally result in wetter (drier) conditions in the WRZ (SRZ), and that a coeval inverse relationship in terms of precipitation amount exists between the two regions, more nuanced scenarios regarding observed variability are being proposed.

To constrain the relationship between CFR climate dynamics and the underlying drivers of the observed variability, we have considered the diatom-based Atlantic sector sea-ice extent and Southern Ocean summer sea-surface temperature (SSST) reconstructions of Nielsen et al. (2004) from marine core TN057-17. Similarities with these records can be observed at sites across the CFR, but it appears that the relationship between humidity and mid-latitude SSSTs changes from positive to negative moving from the eastern to western CFR. At the coastal eastern CFR site of Eilandvlei (Quick et al., 2018), for example, higher percentages of afrotemperate forest pollen (considered to indicate increased humidity and reduced drought stress) correlate well with higher SSSTs at TN057-17 (Fig. 8). In contrast, higher humidity at Pakhuis and Katbakkies passes are more clearly linked to lower SSSTs. Climatically, this most likely indicates that increased westerly influence results in more humid conditions in the lee of the Cederberg mountains, perhaps related to a greater frequency of more powerful frontal systems.

Considering the relationship between the Pakhuis and

Katbakkies pass sites, the impact of changes in westerly influence is variable even between these two sites, despite their proximity and their shared position in the lee of the Cederberg. Katbakkies Pass $\delta^{15}N$ record exhibits changes in both the timing and amplitude that are similar to changes in TN057-17 SSSTs, perhaps indicating that variations in humidity are more tightly coupled to temperate frontal systems than at Pakhuis Pass, where the timing and direction of the anomalies is shared, but the local response is less consistent (Fig. 8). As has been indicated (Chase et al., 2017), increased frontal activity during the Holocene is not necessarily inconsistent with the increases in summer rain that have been previously suggested to drive moisture availability at Katbakkies Pass (Chase et al., 2015b), but it is clear that further work is required to adequately understand how temperate and tropical systems interact to create precipitation events in the region on the timescales considered here.

Underscoring the regional heterogeneity and the variable influence of the region's moisture bearing systems, the Holocene record from De Rif once again is markedly different from the Pakhuis and Katbakkies pass sites (Fig. 8). Whereas the Pakhuis and Katbakkies Pass records exhibit a generally negative relationship between humidity and TN057-17 SSSTs, at De Rif the relationship is generally positive, with more humid conditions occurring during periods of relatively elevated SSSTs. In the early Holocene, while sea ice presence is low in the Atlantic sector of the Southern Ocean, conditions at De Rif are at their most humid for the last 19,400 years. With cooling SSSTs and increased sea ice presence after 7000 cal BP, conditions become significantly drier. This extreme change during the early to mid-Holocene transition exemplifies the apparently sharply contrasting trends across the region, with the records from both Pakhuis and Katbakkies pass showing a strong increase in humidity evident from ~7000 to 6000 cal BP. While more muted, this coeval inverse relationship between the Pakhuis and Katbakkies passes sites and De Rif persists throughout the Holocene, indicating that conditions at all of the sites are controlled by a shared dynamic, but that opposing factors determine conditions in the mountains (De Rif) and the rainshadow (Pakhuis and Katbakkies passes).

Of particular significance is how the opposing responses affect climatic gradients across the region. During the early Holocene, based on the $\delta^{15}N$ data, a very strong hydroclimatic gradient existed along the eastern slope of the Cederberg Mountains (Fig. 9). Following the early to mid-Holocene transition, this gradient became much weaker, with more similar hydroclimatic conditions existing between the western CFR sites considered here. While only the records from De Rif and Pakhuis Pass extend to the Last Glacial Maximum, indications are that these gradients were weakened even further during the late Pleistocene, with similar $\delta^{15}N$ values at both sites suggesting nearly equivalent hydroclimatic conditions.

We hypothesise that these changes in environmental gradients may have had a significant influence on the diversity and distinction of environmental niches in the region, and that changes in

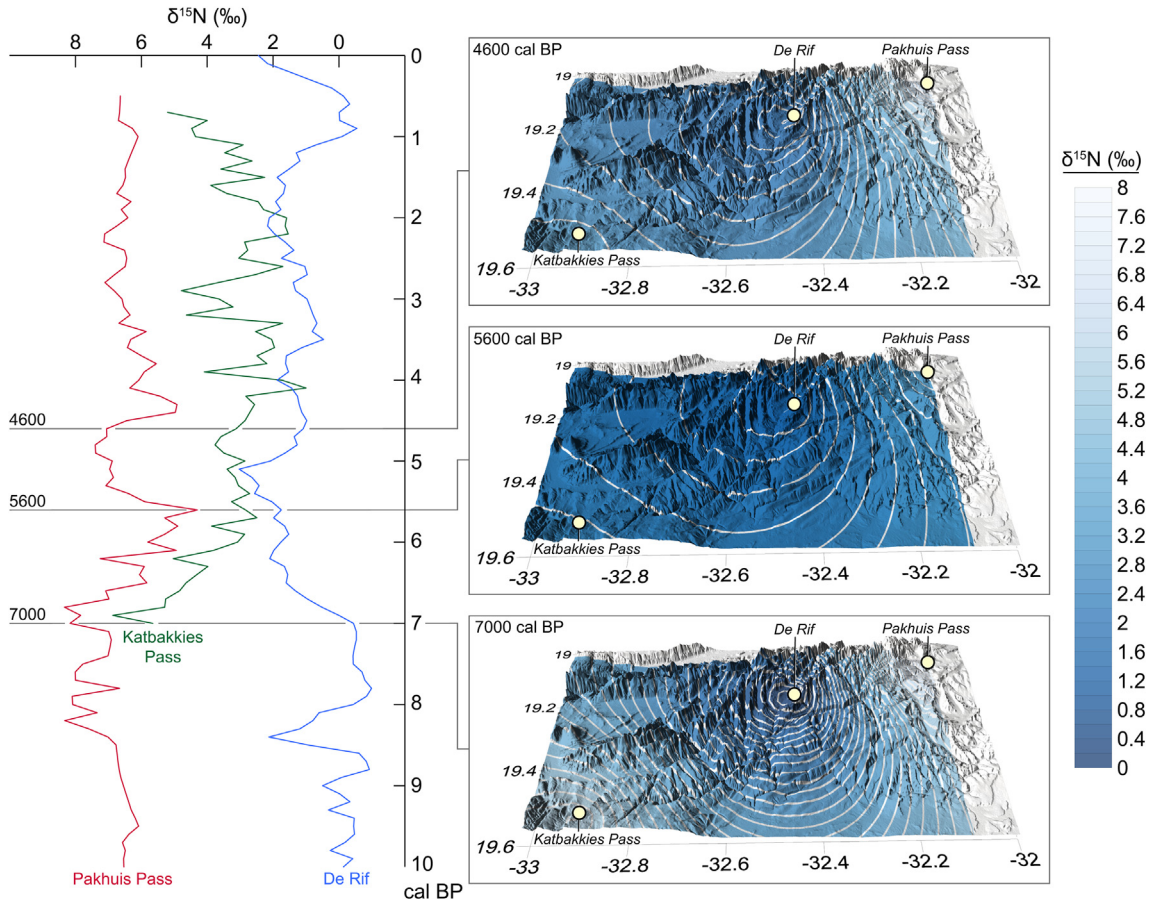

Fig. 9. Holocene western Cape Floristic Region $\delta^{15}N$ records from the Pakhuis Pass (this paper), Katbakkies Pass (Chase et al., 2015b) and De Rif (Chase et al., 2015a) rock hyrax middens, resampled to a common 100-year resolution (linear interpolation). Three time slices have been selected across the mid-Holocene (4600, 5600 and 7000 cal BP), and the $\delta^{15}N$ values from the sites, as proxies for water availability, have been used to interpolate the steepness of hydroclimatic ($\delta^{15}N$) gradients between the sites. White isolines are described at 0.2‰ $\delta^{15}N$ intervals. Note, as only three sites were used in this calculation, extrapolated gradients not along the vector described by these three sites should not be considered as reliable reconstructions.

these gradients may have acted as locks for gene flow, serving to alternatively isolate or enable the migration and mixing of plant species across the region. Considering the observation that species richness in the western CFR is higher in montane regions, the data presented here provide palaeoclimatic evidence that highly variable spatial environmental gradients may have acted as a kind of allopatric speciation pump (e.g. Goldblatt and Manning, 2002; Haffer, 1969; Linder, 1985; Linder, 2003; Verboom et al., 2015), with the repeated isolation and mixing promoting the exceptionally high species diversity of the CFR.

Further work will be required to establish where and to what extent variability on the scale discussed in this paper has been biologically significant. Has the degree or rate of change exceeded the tolerance of specific plant species or their ability to migrate? Can the spatial configuration of climate response anomalies be reliably linked to spatial patterns of species richness? Or, are the changes observed in the records discussed largely insignificant, and play no consequential role in determining species richness? Studies of fossil pollen records from the region provide a mixed response, with some indicating only minor changes in vegetation composition during the late Pleistocene and Holocene (Meadows et al., 2010; Meadows and Sugden, 1991), while others indicate substantial changes in vegetation (Scott and Woodborne, 2007a; Valsecchi et al., 2013). To adequately evaluate and compare these findings, more sites from transects across the region will need to be studied using a consistent methodology that employs a range of proxies capable of differentiating climate and vegetation change, and assessing spatial patterns of genetic diversity.

5. Conclusions

- We present a new, high resolution $\delta^{15}N$ record from Pakhuis Pass in the Cederberg Mountains of the western Cape Floristic Region.
- Like recently published records from the region (Chase et al., 2015a, 2015b), the data from Pakhuis Pass indicate substantial, rapid changes in hydroclimatic conditions, contrasting with earlier suggestions that the Cederberg experienced relatively little environmental change during since the LGM (Meadows et al., 2010; Meadows and Sugden, 1991).
- The record from Pakhuis Pass indicates similarities with patterns of change observed in comparable records from Katbakkies Pass ((Chase et al., 2015b), also in the rainshadow of the Cederberg) but contrasts sharply with conditions at De Rif (Chase et al., 2015a), where a coeval inverse pattern of variability is observed. Commonalities in the *timing* of change suggest a shared driver of regional climate dynamics, but distinct local responses, perhaps as a function of orographic influences.
- The opposing regional responses indicate significant changes in environmental gradients across the western CFR.
- While hydroclimatic conditions at Pakhuis Pass and De Rif may have been similar immediately after the LGM, subsequent responses to changes in global boundary conditions during deglaciation resulted in the establishment of a steep environmental gradient between the sites.
- We hypothesise that changes in the slope of this gradient likely reflect similar patterns across the region, and that these changes may have driven an allopatric speciation pump, contributing to the elevated species diversity observed in the montane regions of the western CFR.
- The spatial heterogeneity of hydroclimatic conditions suggested by the data included in this study indicates the need for more sites and comparable data from across the CFR in order to resolve the complexity of response to long-term climate change.

Acknowledgements

The research leading to these results has received funding from the European Research Council under the European Union's Seventh Framework Programme (FP7/2007–2013), ERC Starting Grant "HYRAX", grant agreement no. 258657. We are very grateful to Louis Scott for providing a portion of the PK1173 midden for analysis. This contribution is number ISEM 2019-138.

Appendix A. Supplementary data

Supplementary data associated with this article can be found, in the online version, at https://doi.org/10.1016/j.quascirev.2019.07.006.

References

Amundson, R., Austin, A.T., Schuur, E.A.G., Yoo, K., Matzek, V., Kendall, C., Uebersax, A., Brenner, D., Baisden, W.T., 2003. Global patterns of the isotopic composition of soil and plant nitrogen. Glob. Biogeochem. Cycles 17.
Austin, A.T., Vitousek, P.M., 1998. Nutrient dynamics on a precipitation gradient in Hawai'i. Oecologia 113, 519–529.
Blaauw, M., 2010. Methods and code for 'classical' age-modelling of radiocarbon sequences. Quat. Geochronol. 5, 512–518.
Blaauw, M., Christen, J.A., 2011. Flexible paleoclimate age-depth models using an autoregressive gamma process. Bayesian Anal. 6, 457–474.
Carr, A.S., Chase, B.M., Boom, A., Medina-Sanchez, J., 2016. Stable isotope analyses of rock hyrax faecal pellets, hyraceum and associated vegetation in southern Africa: implications for dietary ecology and palaeoenvironmental reconstructions. J. Arid Environ. 134, 33–48.
Chase, B.M., Boom, A., Carr, A.S., Carré, M., Chevalier, M., Meadows, M.E., Pedro, J.B., Stager, J.C., Reimer, P.J., 2015a. Evolving southwest African response to abrupt deglacial North Atlantic climate change events. Quat. Sci. Rev. 121, 132–136.
Chase, B.M., Boom, A., Carr, A.S., Meadows, M.E., Reimer, P.J., 2013. Holocene climate change in southernmost South Africa: rock hyrax middens record shifts in the southern westerlies. Quat. Sci. Rev. 82, 199–205.
Chase, B.M., Chevalier, M., Boom, A., Carr, A.S., 2017. The dynamic relationship between temperate and tropical circulation systems across South Africa since the last glacial maximum. Quat. Sci. Rev. 174, 54–62.
Chase, B.M., Lim, S., Chevalier, M., Boom, A., Carr, A.S., Meadows, M.E., Reimer, P.J., 2015b. Influence of tropical easterlies in southern Africa's winter rainfall zone during the Holocene. Quat. Sci. Rev. 107, 138–148.
Chase, B.M., Meadows, M.E., 2007. Late Quaternary dynamics of southern Africa's winter rainfall zone. Earth Sci. Rev. 84, 103–138.
Chase, B.M., Meadows, M.E., Carr, A.S., Reimer, P.J., 2010. Evidence for progressive Holocene aridification in southern Africa recorded in Namibian hyrax middens: implications for African Monsoon dynamics and the "African Humid Period". Quat. Res. 74, 36–45.
Chase, B.M., Meadows, M.E., Scott, L., Thomas, D.S.G., Marais, E., Sealy, J., Reimer, P.J., 2009. A record of rapid Holocene climate change preserved in hyrax middens from southwestern Africa. Geology 37, 703–706.
Chase, B.M., Quick, L.J., Meadows, M.E., Scott, L., Thomas, D.S.G., Reimer, P.J., 2011. Late glacial interhemispheric climate dynamics revealed in South African hyrax middens. Geology 39, 19–22.
Chase, B.M., Scott, L., Meadows, M.E., Gil-Romera, G., Boom, A., Carr, A.S., Reimer, P.J., Truc, L., Valsecchi, V., Quick, L.J., 2012. Rock hyrax middens: a palaeoenvironmental archive for southern African drylands. Quat. Sci. Rev. 56, 107–125.
Chevalier, M., 2019. Enabling possibilities to quantify past climate from fossil assemblages at a global scale. Glob. Planet. Chang. 175, 27–35.
Chevalier, M., Chase, B.M., 2016. Determining the drivers of long-term aridity variability: a southern African case study. J. Quat. Sci. 31, 143–151.
Clark, P.U., Dyke, A.S., Shakun, J.D., Carlson, A.E., Clark, J., Wohlfarth, B., Mitrovica, J.X., Hostetler, S.W., McCabe, A.M., 2009. The last glacial maximum. Science 325, 710–714.
Cockcroft, M.J., Wilkinson, M.J., Tyson, P.D., 1987. The application of a present-day climatic model to the late Quaternary in southern Africa. Clim. Change 10, 161–181.
Cockroft, M.J., Wilkinson, M.J., Tyson, P.D., 1988. A palaeoclimatic model for the late Quaternary in southern Africa. Palaeoecol. Afr. 19, 279–282.
Cowling, R.M., 1992. The Ecology of Fynbos: Nutrients, Fire, and Diversity. Oxford University Press, Cape Town.
Cowling, R.M., Cartwright, C.R., Parkington, J.E., Allsopp, J.C., 1999. Fossil wood charcoal assemblages from Elands Bay Cave, South Africa: implications for Late Quaternary vegetation and climates in the winter-rainfall fynbos biome. J. Biogeogr. 26, 367–378.
Cowling, R.M., Holmes, P.M., Rebelo, A.G., 1992. Plant diversity and endemism. In: Cowling, R.M. (Ed.), Ecology of Fynbos. Nutrients, Fire and Diversity. Oxford University Press, Cape Town, pp. 62–112.
Cowling, R.M., Lombard, A.T., 2002. Heterogeneity, speciation/extinction history and

climate: explaining regional plant diversity patterns in the Cape Floristic Region. Divers. Distrib. 8, 163–179.
Cowling, R.M., Potts, A.J., Bradshaw, P.L., Colville, J., Arianoutsou, M., Ferrier, S., Forest, F., Fyllas, N.M., Hopper, S.D., Ojeda, F., Procheş, Ş., Smith, R.J., Rundel, P.W., Vassilakis, E., Zutta, B.R., 2015. Variation in plant diversity in mediterranean-climate ecosystems: the role of climatic and topographical stability. J. Biogeogr. 42, 552–564.
Cowling, R.M., Richardson, D.M., Schulze, R.J., Hoffman, M.T., Midgley, J.J., Hilton-Taylor, C., 1997. Species diversity at the regional scale. In: Cowling, R.M., Richardson, D.M., Pierce, S.M. (Eds.), Vegetation of Southern Africa. Cambridge University Press, Cambridge, pp. 447–473.
Craine, J.M., Elmore, A.J., Aidar, M.P.M., Bustamante, M., Dawson, T.E., Hobbie, E.A., Kahmen, A., Mack, M.C., McLauchlan, K.K., Michelsen, A., Nardoto, G.B., Pardo, L.H., Peñuelas, J., Reich, P.B., Schuur, E.A.G., Stock, W.D., Templer, P.H., Virginia, R.A., Welker, J.M., Wright, I.J., 2009. Global patterns of foliar nitrogen isotopes and their relationships with climate, mycorrhizal fungi, foliar nutrient concentrations, and nitrogen availability. New Phytol. 183, 980–992.
Diekmann, B., Falker, M., Kuhn, G., 2003. Environmental history of the Southeastern South Atlantic since the Middle Miocene: evidence from the sedimentological records of ODP sites 1088 and 1092. Sedimentology 50, 511–529.
Dynesius, M., Jansson, R., 2000. Evolutionary consequences of changes in species' geographical distributions driven by Milankovitch climate oscillations. Proc. Natl. Acad. Sci. Unit. States Am. 97, 9115–9120.
Fischer, H., Fundel, F., Ruth, U., Twarloh, B., Wegner, A., Udisti, R., Becagli, S., Castellano, E., Morganti, A., Severi, M., Wolff, E., Littot, G., Röthlisberger, R., Mulvaney, R., Hutterli, M.A., Kaufmann, P., Federer, U., Lambert, F., Bigler, M., Hansson, M., Jonsell, U., de Angelis, M., Boutron, C., Siggaard-Andersen, M.-L., Steffensen, J.P., Barbante, C., Gaspari, V., Gabrielli, P., Wagenbach, D., 2007. Reconstruction of millennial changes in dust emission, transport and regional sea ice coverage using the deep EPICA ice cores from the Atlantic and Indian Ocean sector of Antarctica. Earth Planet. Sci. Lett. 260, 340–354.
Forest, F., Grenyer, R., Rouget, M., Davies, T.J., Cowling, R.M., Faith, D.P., Balmford, A., Manning, J.C., Procheş, Ş., van der Bank, M., Reeves, G., Hedderson, T.A.J., Savolainen, V., 2007. Preserving the evolutionary potential of floras in biodiversity hotspots. Nature 445, 757.
GBIF.org, 2018a. Anthocerotopsida Occurrence Data Downloaded on September 13th. GBIF.org.
GBIF.org, 2018b. Cycadopsidae Occurrence Data Downloaded on March 30th. GBIF.org.
GBIF.org, 2018c. Gingkoopsidae Occurrence Data Downloaded on March 30th. GBIF.org.
GBIF.org, 2018d. Gnetopsidae Occurrence Data Downloaded on March 30th. GBIF.org.
GBIF.org, 2018e. Liliopsida Occurrence Data Downloaded on September 13th. GBIF.org.
GBIF.org, 2018f. Lycopodiopsida Occurrence Data Downloaded on September 13th. GBIF.org.
GBIF.org, 2018g. Magnoliopsida Occurrence Data Downloaded on March 30th. GBIF.org.
GBIF.org, 2018h. Pinopsidae Occurrence Data Downloaded on March 30th. GBIF.org.
GBIF.org, 2018i. Polypodiopsida Occurrence Data Downloaded on September 13th. GBIF.org.
Goldblatt, P., 1978. An analysis of the flora of southern Africa: its characteristics, relationships, and origins. Ann. Mo. Bot. Gard. 65, 369–436.
Goldblatt, P., Manning, J.C., 2002. Plant diversity of the Cape region of southern Africa. Ann. Mo. Bot. Gard. 89, 281–302.
Haffer, J., 1969. Speciation in Amazonian forest birds. Science 165, 131–137.
Handley, L.L., Austin, A.T., Stewart, G.R., Robinson, D., Scrimgeour, C.M., Raven, J.A., Heaton, T.H.E., Schmidt, S., 1999. The ^{15}N natural abundance ($\delta^{15}N$) of ecosystem samples reflects measures of water availability. Funct. Plant Biol. 26, 185–199.
Hartman, G., 2011. Are elevated $\delta^{15}N$ values in herbivores in hot and arid environments caused by diet or animal physiology? Funct. Ecol. 25, 122–131.
Hartman, G., Danin, A., 2010. Isotopic values of plants in relation to water availability in the Eastern Mediterranean region. Oecologia 162, 837–852.
Hijmans, R., Cameron, S.E., Parra, J.L., Jones, P.G., Jarvis, A., 2005. Very high resolution interpolated climate surfaces for global land areas. Int. J. Climatol. 25, 1965–1978.
Hogg, A.G., Hua, Q., Blackwell, P.G., Niu, M., Buck, C.E., Guilderson, T.P., Heaton, T.J., Palmer, J.G., Reimer, P.J., Reimer, R.W., Turney, C.S.M., Zimmerman, S.R.H., 2013. SHCal13 southern Hemisphere calibration, 0–50,000 Years cal BP. Radiocarbon 55, 1889–1903.
Killick, R., Fearnhead, P., Eckley, I.A., 2012. Optimal detection of changepoints with a linear computational cost. J. Am. Stat. Assoc. 107, 1590–1598.
Lim, S., Chase, B.M., Chevalier, M., Reimer, P.J., 2016. 50,000 years of vegetation and climate change in the southern Namib Desert, Pella, South Africa. Palaeogeogr. Palaeoclimatol. Palaeoecol. 451, 197–209.
Linder, H.P., 1985. Gene flow, speciation, and species diversity patterns in a species-rich area: the Cape Flora. Species Spec. 4, 53–57.
Linder, H.P., 1991. Environmental correlates of patterns of species richness in the south-western Cape Province of South Africa. J. Biogeogr. 18, 509–518.
Linder, H.P., 2003. The radiation of the Cape flora, southern Africa. Biol. Rev. Camb. Philos. Soc. 78, 597–638.
Linder, H.P., 2005. Evolution of diversity: the Cape flora. Trends Plant Sci. 10, 536–541.
Meadows, M.E., Chase, B.M., Seliane, M., 2010. Holocene palaeoenvironments of the Cederberg and Swartruggens mountains, Western Cape, South Africa: pollen and stable isotope evidence from hyrax dung middens. J. Arid Environ. 74, 786–793.
Meadows, M.E., Sugden, J.M., 1991. A vegetation history of the last 14,000 years on the Cederberg, southwestern Cape Province. South Afr. J. Sci. 87, 34–43.
Mucina, L., Rutherford, M.C., 2006. The Vegetation of South Africa, Lesotho and Swaziland, Strelitzia. South African National Biodiversity Institute, Pretoria.
Murphy, B.P., Bowman, D.M.J.S., 2006. Kangaroo metabolism does not cause the relationship between bone collagen $\delta^{15}N$ and water availability. Funct. Ecol. 20, 1062–1069.
Murphy, B.P., Bowman, D.M.J.S., 2009. The carbon and nitrogen isotope composition of Australian grasses in relation to climate. Funct. Ecol. 23, 1040–1049.
Newsome, S.D., Miller, G.H., Magee, J.W., Fogel, M.L., 2011. Quaternary record of aridity and mean annual precipitation based on $\delta^{15}N$ in ratite and dromornithid eggshells from Lake Eyre, Australia. Oecologia 167, 1151–1162.
Nielsen, S.H.H., Koç, N., Crosta, X., 2004. Holocene climate in the Atlantic sector of the Southern Ocean: controlled by insolation or oceanic circulation? Geology 32, 317–320.
Peri, P.L., Ladd, B., Pepper, D.A., Bonser, S.P., Laffan, S.W., Amelung, W., 2012. Carbon ($\delta^{13}C$) and nitrogen ($\delta^{15}N$) stable isotope composition in plant and soil in Southern Patagonia's native forests. Glob. Chang. Biol. 18, 311–321.
Quick, L.J., Chase, B.M., Meadows, M.E., Scott, L., Reimer, P.J., 2011. A 19.5 kyr vegetation history from the central Cederberg Mountains, South Africa: Palynological evidence from rock hyrax middens. Palaeogeogr. Palaeoclimatol. Palaeoecol. 309, 253–270.
Quick, L.J., Chase, B.M., Wündsch, M., Kirsten, K.L., Chevalier, M., Mäusbacher, R., Meadows, M.E., Haberzettl, T., 2018. A high-resolution record of Holocene climate and vegetation dynamics from the southern Cape coast of South Africa: pollen and microcharcoal evidence from Eilandvlei. J. Quat. Sci. 33, 487–500.
Rehfeld, K., Marwan, N., Heitzig, J., Kurths, J., 2011. Comparison of correlation analysis techniques for irregularly sampled time series. Nonlinear Process Geophys. 18, 389–404.
Roberts, D.L., Neumann, F.H., Cawthra, H.C., Carr, A.S., Scott, L., Durugbo, E.U., Humphries, M.S., Cowling, R.M., Bamford, M.K., Musekiwa, C., MacHutchon, M., 2017. Palaeoenvironments during a terminal Oligocene or early Miocene transgression in a fluvial system at the southwestern tip of Africa. Glob. Planet. Chang. 150, 1–23.
Scott, L., Woodborne, S., 2007a. Pollen analysis and dating of late quaternary faecal deposits (hyraceum) in the Cederberg, western Cape, South Africa. Rev. Palaeobot. Palynol. 144, 123–134.
Scott, L., Woodborne, S., 2007b. Vegetation history inferred from pollen in Late Quaternary faecal deposits (hyraceum) in the Cape winter-rain region and its bearing on past climates in South Africa. Quat. Sci. Rev. 26, 941–953.
Slota, P.J., Jull, A.J.T., Linick, T.W., Toolin, L.J., 1987. Preparation of small samples for ^{14}C accelerator targets by catalytic reduction of CO. Radiocarbon 29, 303–306.
Stute, M., Talma, A.S., 1998. Glacial temperatures and moisture transport regimes reconstructed from noble gas and $\delta^{18}O$, Stampriet aquifer, Namibia. In: Isotope Techniques in the Study of Past and Current Environmental Changes in the Hydrosphere and the Atmosphere. IAEA Vienna Symposium 1997, Vienna, Austria, pp. 307–318.
Talma, A.S., Vogel, J.C., 1992. Late quaternary paleotemperatures derived from a speleothem from Cango Caves, Cape Province, South Africa. Quat. Res. 37, 203–213.
Trabucco, A., Zomer, R.J., 2009. Global aridity Index (Global-Aridity) and global potential evapo-transpiration (Global-PET) Geospatial database. In: Information, C.C.f.S. (Ed.), CGIAR-CSI GeoPortal. http://www.csi.cgiar.org.
Trauth, M.H., Foerster, V., Junginger, A., Asrat, A., Lamb, H.F., Schaebitz, F., 2018. Abrupt or gradual? Change point analysis of the late Pleistocene–Holocene climate record from Chew Bahir, southern Ethiopia. Quat. Res. 1–10.
Tyson, P.D., 1986. Climatic Change and Variability in Southern Africa. Oxford University Press, Cape Town.
Tyson, P.D., Preston-Whyte, R.A., 2000. The Weather and Climate of Southern Africa. Oxford University Press, Cape Town.
UNEP, 1997. World Atlas of Desertification, second ed. United Nations Environment Programme, London.
Valsecchi, V., Chase, B.M., Slingsby, J.A., Carr, A.S., Quick, L.J., Meadows, M.E., Cheddadi, R., Reimer, P.J., 2013. A high resolution 15,600-year pollen and microcharcoal record from the Cederberg Mountains, South Africa. Palaeogeogr. Palaeoclimatol. Palaeoecol. 387, 6–16.
van Zinderen Bakker, E.M., 1976. The evolution of late Quaternary paleoclimates of Southern Africa. Palaeoecol. Afr. 9, 160–202.
Verboom, G.A., Linder, H.P., Forest, F., Hoffman, V., Bergh, N.G., Cowling, R.M., 2014. Cenozoic assembly of the greater Cape flora. In: Allsopp, N., Colville, J.F., Verboom, G.A. (Eds.), Fynbos: Ecology, Evolution and Conservation of a Mega-diverse Region. Oxford University Press, Oxford, pp. 93–118.
Verboom, G.A., Nicola, G.B., Sarah, A.H., Vera, H., Matthew, N.B., 2015. Topography as a driver of diversification in the Cape Floristic region of South Africa. New Phytol. 207, 368–376.
Yamazaki, D., Ikeshima, D., Tawatari, R., Yamaguchi, T., O'Loughlin, F., Neal, J.C., Sampson, C.C., Kanae, S., Bates, P.D., 2017. A high-accuracy map of global terrain elevations. Geophys. Res. Lett. 44, 5844–5853.